Mass movements in small canyons in the northeast of Baiyun deepwater area, north of the South China Sea

LI Xishuang[1], LIU Lejun[1], LI Jiagang[2], GAO Shan[1], ZHOU Qingjie[1], SU Tianyun[1]

[1] The First Institute of Oceanography, State Oceanic Administration, Qingdao 266061, China

[2] Research Center of China National Offshore Oil Corporation, Beijing 100027, China

Abstract

The process of mass movements and their consequent turbidity currents in large submarine canyons has been widely reported, however, little attention was paid to that in small canyons. In this paper, we document mass movements in small submarine canyons in the northeast of Baiyun deepwater area, north of the South China Sea (SCS), and their strong effects on the evolution of the canyons based on geophysical data. Submarine canyons in the study area arrange closely below the shelf break zone which was at the depth of –500 m. Within submarine canyons, seabed surface was covered with amounts of failure scars resulted from past small-sized landslides. A complex process of mass transportation in the canyons is indicated by three directions of mass movements. Recent mass movement deposits in the canyons exhibit translucent reflections or parallel reflections which represent the brittle deformation and the plastic deformation, respectively. The area of most landslides in the canyons is less than 3 km². The trigger mechanisms for mass movements in the study area are gravitational overloading, slope angle and weak properties of soil. Geophysical data indicate that the genesis of submarine canyons is the erosion of mass movements and consequent turbidity currents. The significant effects of mass movements on canyon are incision and sediment transportation at the erosion phases and fillings supply at the fill phases. This research will be helpful for the geological risk assessments and understanding the sediment transportation in the northern margin of the SCS.

Key words: mass movement, geophysical data, trigger mechanism, submarine canyon, north of the South China Sea

1 Introduction

Submarine canyons develop widely in the shelf break zones and their adjacent slopes (Shepard, 1965; Harris and Whiteway, 2011) and they were important passages for sediments transportation and energy exchange from the shelf to the deep water (Inman et al., 1976; Shepard, 1979; Hickey et al., 1986; Xu et al., 2002; Puig et al., 2003; Canals et al., 2006; Allen and Durrieu De Madron, 2009; Vangriesheim et al., 2009; Pierau et al., 2011). As the important sedimentary processes in canyons, mass movements and their consequences are not only the main factors of the formation of canyons (Shepard, 1981; Krastel et al., 2001), but also play a crucial role in their evolution (Farre et al., 1983; Li, 1993; Baztan et al., 2005; Green and Uken, 2008; Li et al., 2012). The process of mass movements and their consequent turbidity currents in large continental margin canyons have been widely reported (Carlson et al., 1991; Khripounoff et al., 2003; Puig et al., 2003; Jenner et al., 2007; Green and Uken, 2008; Arzola et al., 2008; Vangriesheim et al., 2009; Xu et al., 2012), however, mass movements and turbidities in small canyons have attracted little attention.

Dozens of small submarine canyons were found below the modern shelf margin in the northeast of Baiyun deepwater area, north of SCS (Fig. 1b). They arranged closely in a range of about 100 km below the modern shelf break zones. Previous studies on these canyons were based mainly on seismic data and focused particularly on deepwater fan related to canyons (Li et al., 2009; Zhu et al., 2010; Wu et al., 2011; Liu et al., 2011; Lü et al., 2012). In 2010, two geophysical cruises were carried out and multi-beam bathymetry (MB) data, sub-bottom profiles (SBP) and 2D multi-channel seismic (MCS) data were collected. In this paper, we will present and analyze the characteristics, process and mechanism of mass movements in modern canyons, and discuss the effects of mass movements on the evolution of canyons by using of these new geophysical data.

2 General setting

The study area locates in the northern of the SCS, 300 km away from the modern coastline, and covers the shelf break zone and the upper-middle slope with water depth ranging from –200 m to –2 000 m. A wide and S-shaped relief groove connects the shelf and the abyssal in the southwest of the study area (Fig. 1b). The Paleo-Zhujiang (Pearl) River provided amounts of sediments to the shelf and slope, especially during low stands of sealevel when the study area was only 100 km away from the Paleo-coastline according to simulation result (Yao et al., 2009).

The Baiyun sag is the southern part of the Zhujiang (Pearl)

River Mouth Basin (ZRMB). It was basically in a relatively stable tectonic subsidence stage without significant structural changes since the last phase of the early Miocene when the tectonic extension of the SCS ended (Gong and Li, 1997).
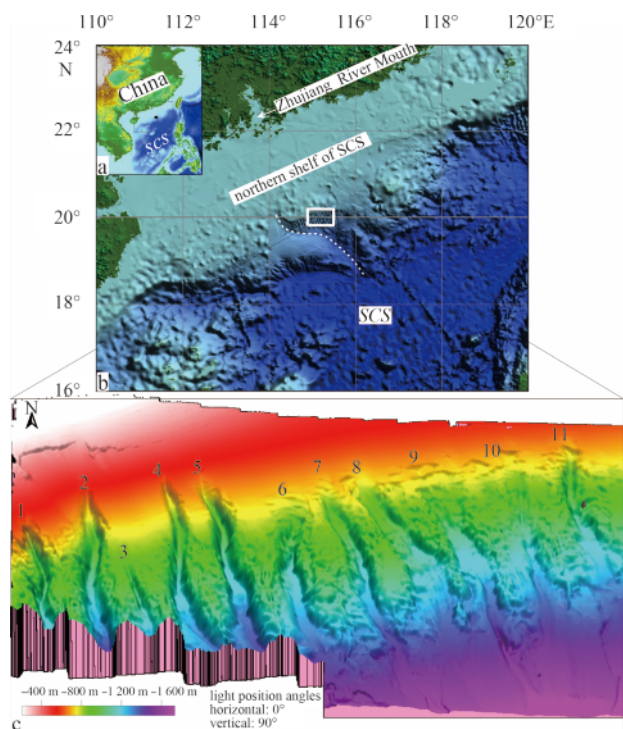
Fig. 1. Inserted map (a) and bathymetric map of the northern South China Sea (b) and 3D surface map of the study area (c). The white dotted line in Fig. 1b shows the location of a wide and S-shaped relief groove nearby the study area; the regional bathymetric map (b) is from USGS Atlas (2005); 3D map of the target area is based on MB data collected in 2010 and the contour interval is 50 m; shelf break line is at water depth of about –500 m; 1, 2,···, 11 is the number of canyons.

Complex ocean dynamic environment exists in the northern SCS, where there are at least 4 main surface currents: the Kuroshio recirculation, the SCS branch of the Kuroshio warm current, the SCS warm current and the Southern China coastal current (Fang et al., 1998), among which, the SCS warm current influences the study area most greatly. Surface water flows to the northeast in summer and the measured maximum velocity ranges from 58 cm/s to more than 100 cm/s (Guan, 1978; Hu et al., 2000).

3 Geophysical dataset

The MB data were collected using of the R/V *NANHAI 503* with a shipborne multi-beam measurement model EM302 in 2010. CARIS software was used to process the data to obtain the Digital Elevation Model (DEM) of 20 m resolution (Fig. 1c). In addition, 500 m × 500 m grid data of water depth in the study area were also collected. During the MB cruise, the SBP survey with penetration depth of 20 to 50 m was conducted synchronously utilizing the shipborne sub-bottom profiler ECHOES 3500. In the seismic cruise in 2010, 150-km-long 2D MCS data were collected. Seismic signals were acquired by a 120-channel digital streamer

with channel spacing of 6.25 m during the survey. The sparker source gave the vertical resolution up to 2 m.

4 Results

4.1 *MB data*

4.1.1 *Topography of modern submarine canyons*

Modern canyons in the Baiyun area arrange closely in the slope where water depth varies from –500 m to –1 700 m (Fig. 2a). The MB data cover 11 of these canyons that spread across a width of 70 km and are numbered 1, 2, ···, 11 respectively from west to east (Fig. 1c). The canyons run from north to south and follow nearly straight paths down the slope. Crossing sections of these canyons show V-type or U-type. For each canyon, the eastern flank is always steeper than the west (Fig. 2b). Channel length ranges from 20 to 30 km and the canyon space varies from 6 km to 7 km. The canyon floors are relatively flat (slope angle < 3°) (Fig. 2c) and their width ranges from 500 m to 1 500 m. The No. 5 canyon can be regarded as a boundary line on whose sides the topography of canyons shows great differences. Canyons on its west side exhibit deep U-type crossing sections and the incision depth is more than 250 m. However, those on the east side are characterized by failure scars with different directions and head bifurcation for some canyons. Channel segments begin at the depth of about –1 400 m.

4.1.2 *Failure Scars*

The seabed, interpreted to represent the shear plane of the past failure, is sub-planar to shallow convex in profile in many cases. Failure scars with different lengths and strikes are found in regions of the canyon heads, the canyon flanks and the platforms between canyons (Fig. 2d). Slope of the failure scars ranges from 5° to 20° (Fig. 2c) and their length varies from hundreds of meters to several kilometers. Most of large scars are parallel to canyon axes and are mainly distributed in canyon flanks. Some small scars parallel to the isobaths are mainly found in the canyon head regions. A small part of scars spread obliquely to canyon axes and develop dominantly in the terraces between canyons.

4.2 *SBP data*

SBP data show large quantities of recent small landslides in the flanks of canyons, the head regions and the platforms between canyons (Fig. 3). The mass movement deposits (MMDs) often exhibit translucent reflections or parallel reflections with middle amplitude and mound, lenticular or wedge shape. The consequent debris flow deposits along the thalwegs are usually characterized by translucent reflection, lenticular shape and clear erosional surface at the bottom. We interpret the MMDs with translucent reflections as the result of sediment plastic deformation which often occurred on the canyon heads and terraces on canyon flanks and the MMDs with parallel reflections and clear shear surfaces as the result of sediment brittle deformation which often occurred on terraces on canyon flanks. More details of acoustic facies are shown in Table 1.

4.3 *2D Ultra high-resolution MCS data*

4.3.1 *Landslides in the canyon head regions*

Periodic landsliding events in shallow sedimentary sequences were revealed by 2D MCS data in the canyon head regions (Fig. 4). The shear planes exhibit slight concaving and have cut sedimentary layers. The slope angle of shear plane ranges
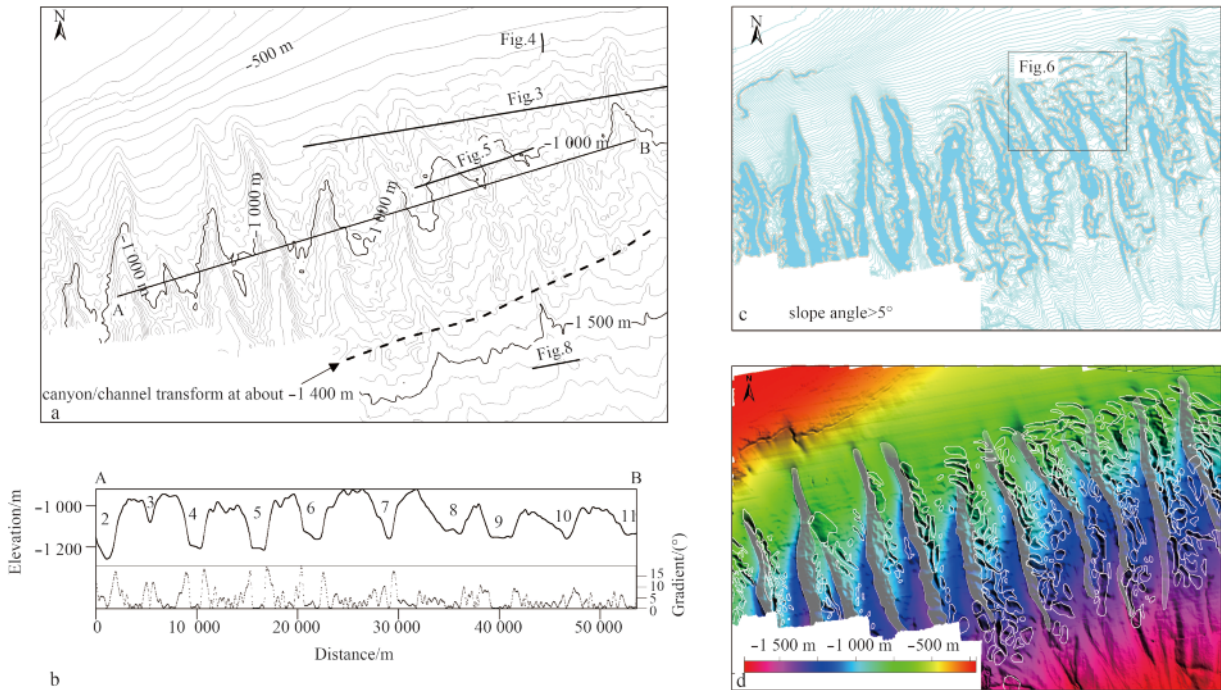
Fig. 2. Bathymetric map of small canyons and failure scars distribution map. a. Contour map of sea floor, b. cross section of canyons, c. steep slope distribution, and d. failure scar distribution. Dash shades in Fig. 2d show the location of western flanks of canyons; white circles in Fig. 2d are landslides identified;these maps are based on MB data.
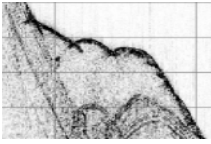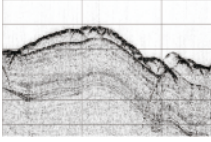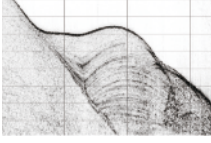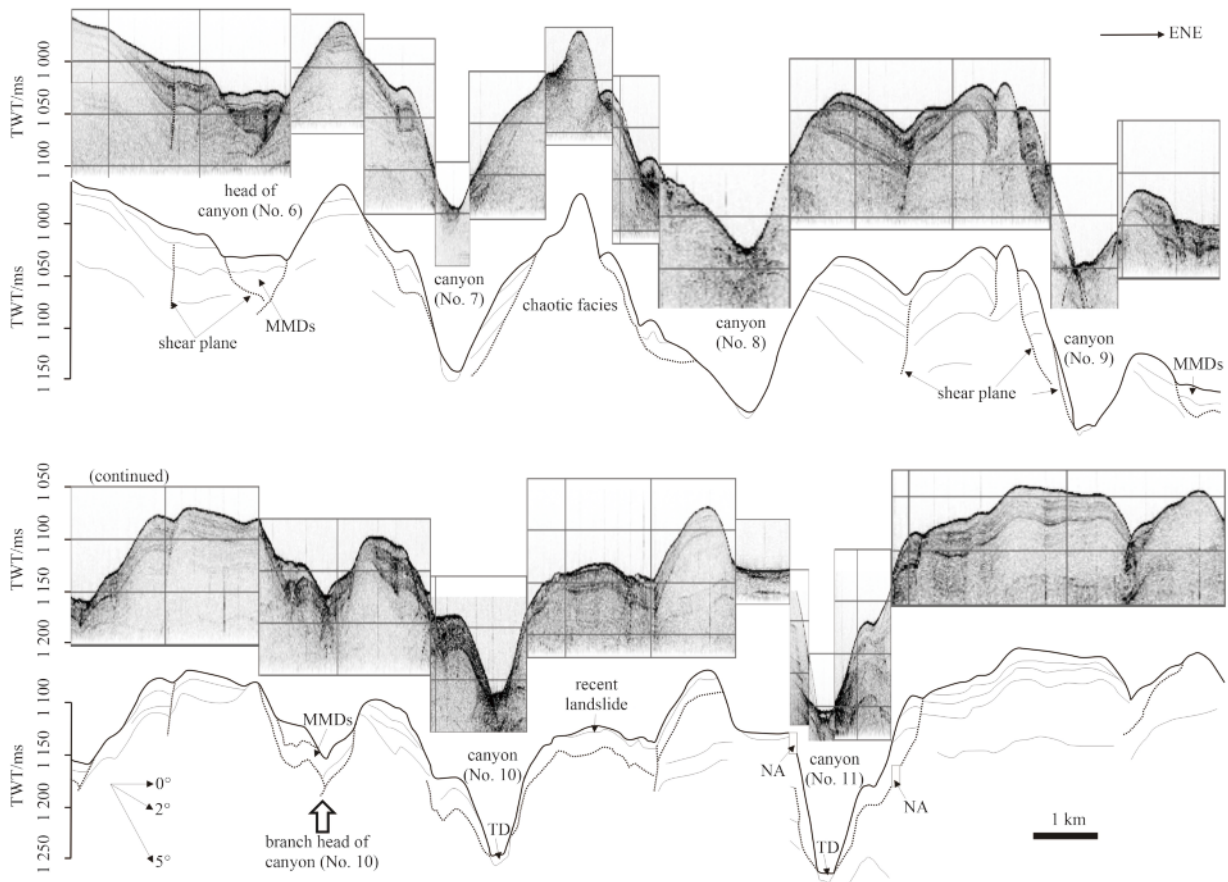

Fig. 3. Acoustic cross section and its interpretation. Line location is in Fig. 2a. MMDs: mass transport deposits; TWT: two way travel time; TD: thalweg deposits; NA: not available; the black dotted lines are shear planes; large amounts of recent landslides develop on canyon flanks.

from 3° to 5°. Seismic facies of deposits indicate that original sedimentary structures were preserved after landsliding. The distance of a recent landsliding is estimated to be 0.5 km based on seismic data.

Table 1. The ratio between coal-bearing

Acoustic images	Acoustic characteristics	Distribution	Interpretation	Classification
	translucent reflection, mound appearance and clear bottom	canyon head, terraces on canyon flank	slump	plastic deformation
	translucent reflection, lenticular or wedge shape and clear bottom	terraces on canyon flank	slump	
	parallel reflection with middle amplitude, lenticular or wedge shape and clear shear plane near the bottom	canyon flank	landslide	brittle deformation
	translucent reflection, lenticular shape and erosional surface at the bottom	canyon floor	debris flow deposits	gravity flow
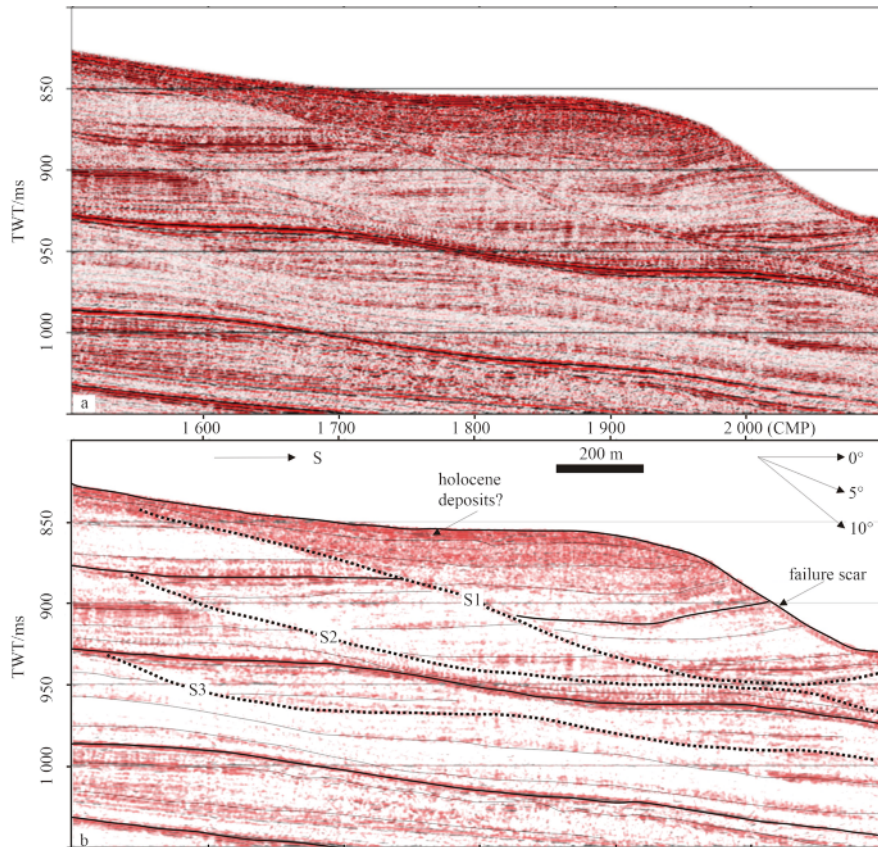
Fig. 4. Seismic data shows landslides in the canyon head region. a. Seismic profile, and b. interpretation. Line location is in Fig. 2a. S1–S3: shear planes; TWT: two way travel time; TRCIDX: trace index; the black dotted lines are shear planes; landslides in different strata show slight concaving.

4.3.2 *Slides in the flanks of canyons*

Many shear planes of ancient mass movements events preserved in the flanks of canyons were revealed by MCS data (Fig. 5). These shear planes are characterized by slight concaving. The slope angle of them ranges from 4° to 9°. Most of landslides on the flanks of canyons show chaotic seismic facies indicating a relatively rapid landsliding process contrasting to that in the canyon head regions.
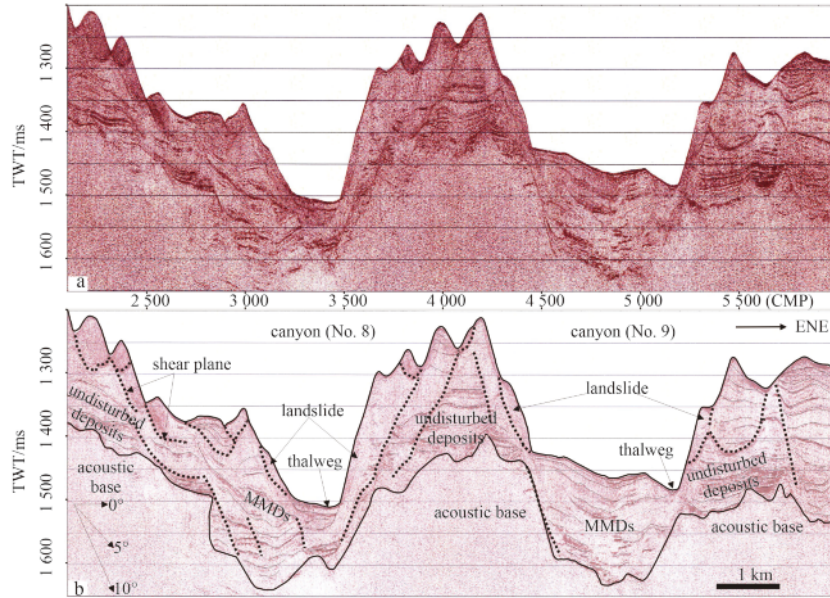

Fig. 5. Seismic architecture cross-cutting modern canyons. a. Seismic profiles, b. interpretation. Line location is in Fig. 2a. TWT: two way travel time; TRCIDX: trace index; MMDs: mass movement deposits.

5 Discussion

5.1 *Mass transportation indicated by failure scars*

Failure scars are usually correlated with mass movement and formed after landsliding (Bugge et al., 1988; Bøe et al., 2000; Dai and Lee, 2002). Most of scars identified in topographic map (Fig. 2d) are certified as failure scars resulted from landsliding by SBP data (Fig. 6). We estimate the size of landslides from areas of failure scars. Statistic results given in Table 2 show that sliding area of most landslides is less than 3 km². SBP indicates that the thickness of most landslides is usually less than 40 m.

Three main directions of mass transportation in canyons are inferred the stretch of failure scars. One is perpendicular to the canyon axis, one is parallel to the canyon axis and the other is oblique to the canyon axis. This indicates a complex process and a route of mass transportation from the sidewall to the canyon floor. We speculate three possible cases of the process of sediments transportation (Fig. 7). In the first case which usually occurred in the canyon head region, sedimentary mass in the sidewall were transported directly to the canyon floor after sliding. In the second case, sedimentary mass were transported many times in the flank of the canyon and finally deposited at the canyon floor. The direction of sediments transportation is perpendicular or oblique to the canyon axis. In the final case, sediments were transported firstly downward along the slope, and then moved perpendicularly or obliquely to the canyon axis.

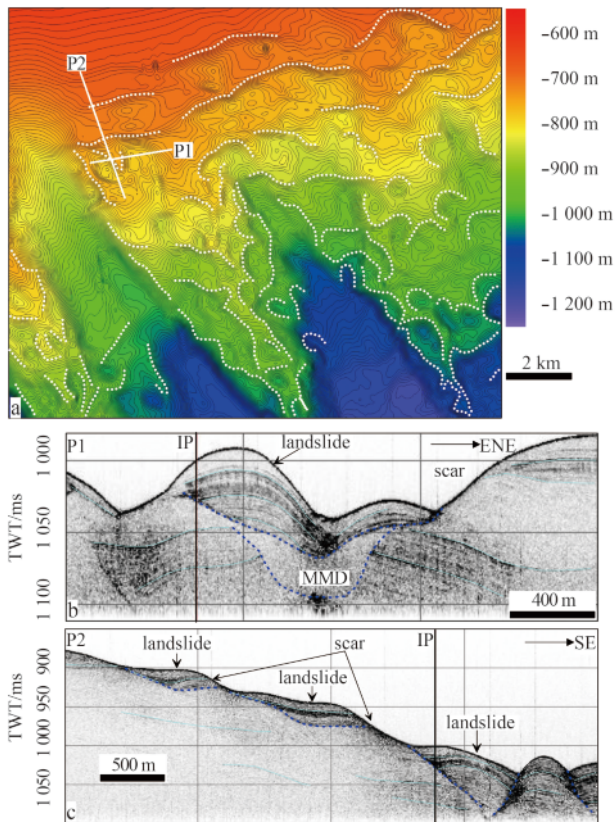### 5.2 *Trigger mechanisms for mass movements*

Earthquakes were often considered as the main trigger mechanism for mass movements in continental margins (Heezen and Ewing, 1952; Belloni and Morris, 1991; Walsh and Martill, 2006; Okada et al., 2008). But in the study area, the seismic activity is very low (Liu et al., 2002). This means the earthquake is not the main trigger mechanism for past mass movements events in the study area. Typhoons events cause extremes in currents and waves in the South China Sea (Chu and Cheng, 2008; Liu et al., 2011), but their depth of influence is typically confined to water depths of 200 m or shallower. Therefore typhoon-induced motion within the water column is not expected to have a direct impact on the sediments within the canyons.

Periodic sliding events in the shelf break zone revealed by MCS data (Fig. 5) indicate that these landslides are related to characteristics and properties of sediment itself. The shelf break zone in the study area was supplied with sediments with high rate, especially during the low sea-level periods (Huang and Wang, 2007). Sediments were mainly made up of high plasticity silts and clays. Therefore, gravitational overloading was the main reason for mass movements in the shelf break zone, where the heads of submarine canyons are located. Within the canyon, especially in the flanks, our slope stability analysis using numerical simulation shows that the high slope angle (up to 20°) and weak properties of soil are considered as main causes of mass movements. When turbidity currents in the canyon floor became more active, unbalance of stress of sediments caused by erosion effect (Embley and Jacobi, 1977) might be the trigger for some landslides in the canyon flanks revealed by MCS data (Fig. 5).

Table 2. Statistics of sliding area in the study area

Sliding area/km²	Counts
0.1–0.5	152
0.5–1.0	83
1.0–3.0	134
3.0–5.0	14
>5.0	7

Fig. 6. Architectures of landslides and associated failure scars. a. Distribution map of scars identified with bathymetric map; the location of enlargement map shows in Fig. 2c; b and c. sub-bottom profiles and their interpretation; the location of sub-bottom profiles show in Fig. 6a; TWT: two way travel time; MMD: mass movement deposit; IP: intersection point of sub-bottom profiles; blue dotted line are shear plane; white dotted curves are upper margins of failure scars.

5.3 *Origin of the canyons*

Erosion of mass movements and consequent turbidity currents was the main cause for the genesis of submarine canyons in continental margins (Shepard, 1979; Harris and Whiteway, 2011), such as the U.S. Middle Atlantic continental margin (Farre et al., 1983) and Australian margin (Heap and Harris, 2008). High deposition rate made fine grained sediments dominating the shelf break zone in the Baiyun deepwater area unstable and thus sediments landsliding would occur. Large amounts of landslides in these canyon heads and the flanks revealed by SBP data indicate that submarine canyons in the study area were related to the sculpture of mass movements and their consequent turbidity currents. Topographical features, such as some of these canyons having second or third tributaries in their upper reaches, also inferred that submarine canyons have an erosion origin. Moreover, extension directions of submarine canyons are different from that of Neogene faults in the study area (Sun et al., 2008), which indicates that submarine canyons were not originated from faults. Our result is consistent with the results of Zhu et al. (2010) and Lü et al. (2012) based on MCS data.

### 5.4 *Effects of mass movement on the evolution of canyons*

Modern submarine canyons in the study area started at the middle Miocene and have suffered multi erosion-fill cycles (Zhu et al., 2010; Lü et al., 2012). Mass movements and consequent turbidity currents played a key role on the evolution of them. At the erosion phases, the sea level was low and the coastline advanced to the ocean. Mass movements become more active due to higher rate supply of sediments in the shelf break zone. Many deepwater fans developing during the low sea-level periods (Pang et al., 2007) inferred that most of sediment after sliding or slumping was transported by turbidity currents to canyon exit and accumulated fans and submarine canyons were the main passages for sediments at the erosion phase. The turbidity current were strong enough to wash away MMDs in the canyon floor and even parts of early fill in the canyon floor might be eroded and transported to the lower, the canyons would be deeply carved and widen. Moreover, more turbidity currents would steeper the flank and trigger more mass movements.

At the fill phases, corresponding to high sea-level stages, the coastlines advanced to the land and sediments supplied to the shelf break zone reduced (Peng et al., 2006; Huang and Wang, 2007). There were no palpable depositional fans in exits of modern canyons (Fig. 8), which indicates that there were no large amounts of sediments transported through canyons. The seismic profile crossing canyon segments shows thick sedimentary fill that suggests most of sediments transported by mass movements and consequent debris flow were mainly trapped and filled in the canyon floors, while in the exits of the canyons, thin sedimentary fill indicates that only small parts of sediments were transported to the exit and the lower area of the canyon by turbidity currents. Mass movements were still active, but the size and the quantity of landslides or slumps would be smaller than that at the erosion phase. That would be favor of reservation of MMDs in canyons.
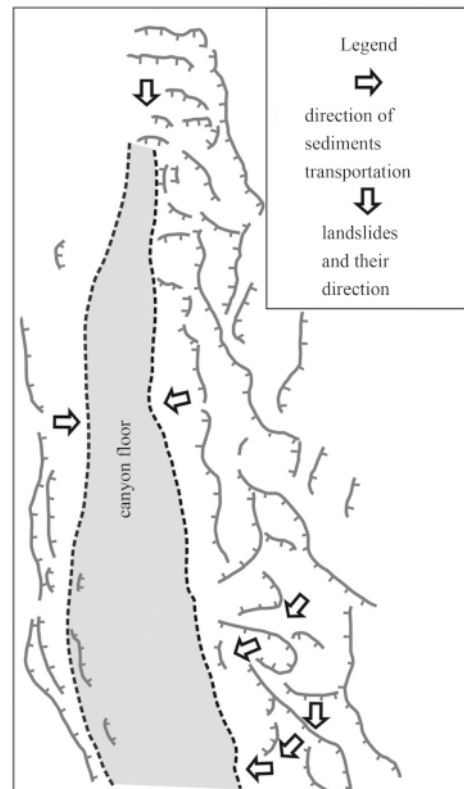
Fig. 7. Skelton map of sediments transportation route indicated by failure scars.
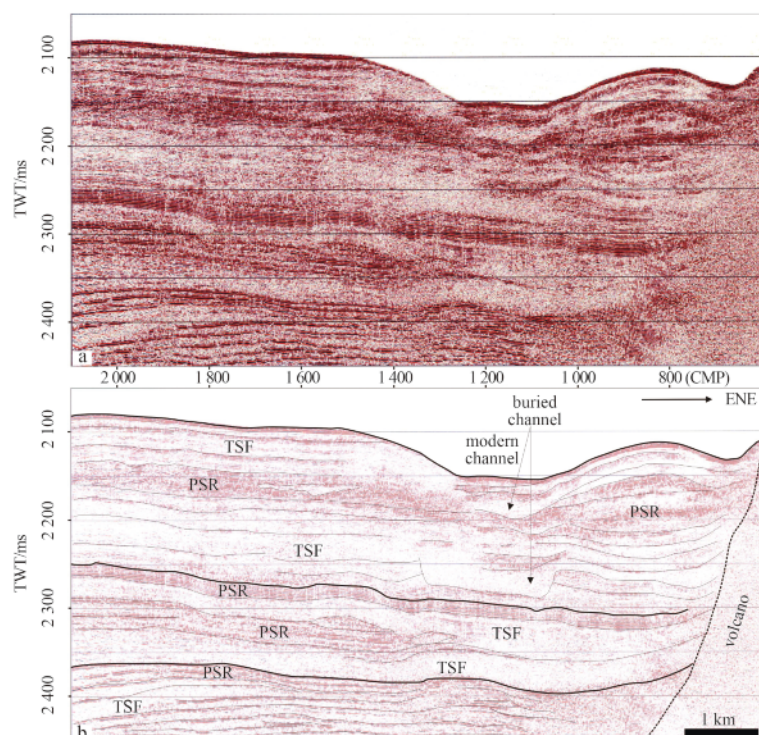
Fig. 8. Seismic architecture of channel segment. a. seismic profiles, b. interpretation. Line location is in Fig. 2a. TWT: two way travel time; TRCIDX: trace index; TSF: translucent seismic face interpreted as turbidite depositss; PSR: parallel seismic reflection interpreted as abysmal deposits; the black dotted lines are shear planes.

In the study area, canyon channel migration has been observed and discussed in several papers (Zhu et al., 2010; Lü et al., 2012; Li et al., 2013; He et al., 2014), but the reason why all channel migrated northeastwards since the middle Miocene is still debated. The high-resolution MCS profiles show that more MMDs with discontinuous parallel reflections were preserved in the eastern flanks and the eastern parts of the floors at the fill phases. Down-slope gravity flow along the canyon axis was not enough to wash away the MMDs and would have to be rerouted eastwards until the end of the fill phase. But at the erosion phases, MMDs would not be preserved in the canyon floors because of strong down-slope gravity flow along the channels. Therefore, eastward migration of canyon channels manly occurred at the fill phases.

6 Conclusions

Large quantities of small-sized mass movements, of which the landsliding area is less than 3 km², were identified with geophysical data within submarine canyons in the Baiyun deepwater area, north of the SCS. Landsliding directions indicate a complex process of sediments transportation from the canyons wall to the floor. Our analysis shows that gravitational overloading, slope angle and weak properties of soil are the leading causes for these small-sized mass movements. Submarine canyons are mainly caused by the erosion of mass movements and consequent turbidity currents. The influence of mass movements on submarine canyons is strong incision during low sea-level stages, which is different from filling of canyons during high sea-level stages.

References

Allen S E, Durrieu De Madron X. 2009. A review of the role of submarine canyons in deep-ocean exchange with the shelf. Ocean Science, 5: 607–620

Arzola R G, Wynn R B, Lastras G, et al. 2008. Sedimentary features and processes in the Nazaré and Setúbal submarine canyons, west Iberian margin. Marine Geology, 250(1–2): 64–88

Baztan J, Berné S, Olivet J- L, et al. 2005. Axial incision: the key to understand submarine canyon evolution (in the western Gulf of Lion). Marine and Petroleum Geology, 22(6–7): 805–826

Belloni L, Morris D. 1991. Earthquake-induced shallow sildes in volcanic debris soils. Geotechnique, 41(4): 539–551

Bøe R, Hovland M, Instanes A, et al. 2000. Submarine slide scars and mass movements in Karmsundet and Skudenesfjorden, southwestern Norway: morphology and evolution. Marine Geology, 167(1–2): 147–165

Bugge T, Belderson R H, Kenyon N H. 1988. The storegga slide. Philosophical Transactions of the Royal Society of London A: Mathematical Physical & Engineering Sciences, 325(1586): 357–388

Canals M, Puig P, Durrieu De Madron X, et al. 2006. Flushing submarine canyons. Nature, 444 (7117): 354–357

Carlson P R, Karl H A, Edwards B D. 1991. Mass sediment failure and transport features revealed by acoustic techniques, Beringian Margin, Bering Sea, Alaska. Marine Geotechnology, 10(1–2): 33–51

Chu P C, Cheng Kuofeng. 2008. South China Sea wave characteristics during typhoon Muifa passage in winter 2004. Journal of Oceanography, 64(1): 1–21

Dai Fuchu, Lee C F. 2002. Landslides on natural terrain. Mountain Research and Development, 22(1): 40–47

Embley R W, Jacobi R D. 1977. Distribution and morphology of large submarine sediment slides and slumps on Atlantic continental margins. Marine Geotechnology, 2(1–4): 205–228

Fang Guohong, Fang Wendong, Fang Yue, et al. 1998. A survey of studies on the South China Sea upper ocean circulation. Acta Oceanographica Taiwanica, 37: 1–16

Farre J A, McGregor B A, Ryan W B F, et al. 1983. Breaching the shelf-break: passage from youthful to mature phase in submarine canyon evolution. In: Stanley D J, Moore G T, eds. The Shelf-break: Critical Interface on Continental Margins. America: Society of Economic Paleontologists and Mineralogists Special Publication, 33: 25–39

Green A, Uken R. 2008. Submarine landsliding and canyon evolution for the northern KwaZulu-Natal continental shelf, South Africa, SW Indian Ocean. Marine Geology, 254(3–4): 152–170

Gong Zaisheng, Li Sitian. 1997. Continental Margin Basin Analysis and Hydrocarbon Accumulation of the Northern South China Sea (in Chinese). Beijing: Science Press, 63–75

Guan Bingxian. 1978. The South China Sea warm current—a winter counter-wind current in the open sea off the Guangdong coast. Oceanology and Limnology Sinica (in Chinese), 9: 117–127

Harris P T, Whiteway T. 2011. Global distribution of large submarine canyons: geomorphic differences between active and passive continental margins. Marine Geology, 285(1–4): 69–86

He Ye, Zhong Guangfa, Wang Liaoliang, et al. 2014. Characteristics and occurrence of submarine canyon-associated landslides in the middle of the northern continental slope, South China Sea. Marine and Petroleum Geology, 57: 546–560

Heap A, Harris P T. 2008. Geomorphology of the Australian margin and adjacent sea floor. Australian Journal of Earth Science, 55(4): 555–585

Heezen B C, Ewing M. 1952. Turbidity currents and submarine slumps, and the 1929 Grand Banks earthquake. America Journal of Science, 250: 849–873

Hickey B, Baker E, Kachel N. 1986. Suspended particle movement in and around Quinault submarine canyon. Marine Geology, 71(1–2): 35–83

Hu Jianyu, Kawamura H, Hong Huasheng, et al. 2000. A review on the currents in the South China Sea: seasonal circulation, South China Sea warm current and Kuroshio intrusion. Journal of Oceanography, 56(6): 607–624

Huang Wei, Wang Pinxian. 2007. Accumulation rate characterstics of deep-water sedimentation in the South China Sea during the last galciation and the Holocene. Haiyang Xuebao (in Chinese), 29(5): 69–73

Inman L, Nordstrom C E, Flick R E. 1976. Currents in submarine canyons: an air-sea-land interaction. Annual Rev Fluid Mechanics, 8: 275–310

Jenner K A, Piper D J W, Campbell D C, et al. 2007. Lithofacies and origin of Late Quaternary mass transport deposits in submarine canyons, central Scotian Slope, Canada. Sedimentology, 54(1): 19–38

Khripounoff A, Vangriesheim A, Babonneau N, et al. 2003. Direct observation of intense turbidity current activity in the Zaire submarine valley at 4000 m water depth. Marine Geology, 194(3–4): 151–158

Krastel S, Schmincke H-U, Jacobs C L, et al. 2001. Submarine landslides around the Canary Islands. Journal of Geophysical Research: Solid Earth (1978–2012), 106(B3): 3977–3997

Li C. 1993. Crescent-shaped slab slides in a submarine canyon system, Arequipa fore-arc basin off southern Peru. Marine Georesources and Geotechnology, 11: 333–346

Li Gang, Piper D J W, Campbell D C, et al. 2012. Turbidite deposition and the development of canyons through time on an intermittently glaciated continental margin: the Bonanza Canyon system, offshore eastern Canada. Marine and Petroleum Geology, 29(1): 90–103

Li Lei, Wang Yingmin, Zhang Lianmei, et al. 2009. Sedimentary sequence and evolution of submarine channel-lobe in Baiyun deepwater area, northern South China Sea. Marine Geology

and Quaternary Geology (in Chinese), 29(4): 71–76

Li Hua, Wang Yingmin, Zhu Weilin, et al. 2013. Seismic characteristics and processes of the Plio-Quaternary unidirectionally migrating channels and contourites in the northern slope of the South China Sea. Marine and Petroleum Geology, 43: 370–380

Liu Jun, Pang Xiong, Yan Chengzhi, et al. 2011. 13.8 Ma deep-water fan deposit in the Baiyun sag on the north continental slope of South China Sea. Special Oil and Gas Reservoirs (in Chinese), 18(4): 39–42

Liu Zhaoshu, Zhao Huanting, Fan Shiqing, et al. 2002. Geology of the South China Sea (in Chinese). Beijing: Science Press, 72

Lü Caili, Yao Yongjian, Gong Yuehua, et al. 2012. Deepwater canyons reworked by bottom currents: sedimentary evolution and genetic model. Journal of Earth Science, 23(5): 731–743

Okada Y, Ochiai H, Kurokawa U, et al. 2008. A channelised long run-out debris slide triggered by the Noto Hanto Earthquake in 2007, Japan. Landslides, 5(2): 235–239

Pang Xiong, Chen Changmin, Peng Dajun, et al. 2007. Sequence stratigraphy of deep-water fan system of pearl River, South China Sea. Earth Science Frontiers (in Chinese), 14(1): 220–229

Peng Dajun, Pang Xiong, Chen Changmin, et al. 2006. The characteristics and controlling factors for the formation of deep-water fan system in south China sea. Acta Sedimentologica Sinica (in Chinese), 24(1): 10–18

Pierau R, Henrich R, Preiß-Daimler I, et al. 2011. Sediment transport and turbidite architecture in the submarine Dakar Canyon off Senegal, NW-Africa. Journal of African Earth Sciences, 60(3): 196–208

Puig P, Ogston A S, Mullenbach B L, et al. 2003. Shelf-to-canyon sediment-transport processes on the Eel continental margin (northern California). Marine Geology, 193(1–2): 129–149

Shepard F P. 1965. Types of submarine valleys. American Association of Petroleum Geologists Bulletin, 49(3): 304–310

Shepard F P. 1979. Currents in submarine canyons and other types of sea valleys. SEPM Special Publications, 27: 85–94

Shepard F P. 1981. Submarine Canyons: multiple causes and long-time persistence. American Association of Petroleum Geologists Bulletin, 65(6): 1062–1077

Sun Longtao, Zhou Di, Chen Changmin, et al. 2008. Fault structures and evolution of Baiyun Sag in Pearl River Mouth Basin. Journal of Tropical Oceanography (in Chinese), 27(2): 25

Vangriesheim A, Khripounoff A, Crassous P. 2009. Turbidity events observed in situ along the Congo submarine channel. Deep-Sea Research Part II: Topical Studies in Oceanography, 56(23): 2208–2222

Walsh S A, Martill D M. 2006. A possible earthquake-triggered megaboulder slide in a Chilean Mio-Pliocene marine sequence: evidence for rapid uplift and bonebed genesis. Journal of the Geological Society, 163(4): 697–705

Wu Jiapeng, Wang Yingmin, Xu Qiang. 2011. A depositional model of submarine canyons in Baiyun sag, Pear River Mouth Basin. Marine Geology Frontiesr (in Chinese), 27(8): 26–31

Xu J P, Barry J P, Paull C K. 2012. Small-scale turbidity currents in a big submarine canyon. Geology, 41(2): 143–146

Xu J P, Noble M, Eittreim S L, et al. 2002. Distribution and transport of suspended particulate matter in Monterey Canyon, California. Marine Geology, 181(1–3): 215–234

Yao Yantao, Harff J, Meyer M, et al. 2009. Reconstruction of paleo-coastlines for the northwestern South China Sea since the Last Glacial Maximum. Science in China (Series D: Earth Sciences), 52(8): 1127–1136

Zhu Mangzheng, Graham S, Pang Xiong, et al. 2010. Characteristics of migrating submarine canyons from the middle Miocene to present: implications for paleoceanographic circulation, northern South China Sea. Marine and Petroleum Geology, 27(1): 307–319